

NLO QCD effects on angular observables in single Higgs production at electron-proton collider

Pramod Sharma,^{a,*} Biswajit Das^b and Ambresh Shivaji^a

^aDepartment of Physical Sciences, Indian Institute of Science Education and Research Mohali, Knowledge city, Sector 81, Manauli, PO, Sahibzada Ajit Singh Nagar, Punjab, India, 140306

^bThe Institute of Mathematical Sciences,
4th Cross St, CIT Campus, Taramani, Chennai, Tamil Nadu, India, 600113
E-mail: ph19010@iisermohali.ac.in, biswajitd@imsc.res.in,
ashivaji@iisermohali.ac.in

Properties of the Higgs boson (H) at current and future particle colliders are crucial to explore new physics beyond the standard model. In particular, experimental and theoretical outlooks at future colliders drive interest in Higgs to gauge boson couplings. Single Higgs production via vector-boson fusion allows probing Higgs couplings with massive vector bosons ($V = W, Z$). We consider electron-proton (eP) collider to study these couplings due to the low background. In a recent study, we considered the most general anomalous Higgs-vector boson (HVV) couplings and explored the potential of eP collider in constraining the parameters of HVV couplings. Our results were based on leading order predictions in perturbation theory. We include further Next to Leading Order (NLO) corrections of Quantum Chromodynamic (QCD) in Standard Model signal to make precise predictions. In this talk, I will present the effect of NLO QCD corrections on the standard model and anomalous HVV couplings.

42nd International Conference on High Energy Physics (ICHEP2024)
18-24 July 2024
Prague, Czech Republic

*Speaker

1. Introduction

The scalar boson with a mass of 125 GeV, discovered by the ATLAS and CMS collaborations at the Large Hadron Collider (LHC) [1, 2], is consistent with the Standard Model (SM) Higgs boson. The SM has demonstrated remarkable success in explaining a wide range of experimental measurements. The investigation of electroweak symmetry breaking via the Higgs-to-vector boson couplings (HVV) is important for new physics searches at current and future colliders. The HVV couplings in the Kappa framework have been measured with an accuracy of 7-8% by CMS [3] and ATLAS [4] using Run-II LHC data. The new physics allowed by such a measurement can be parametrized by the most general Lorentz structure of two rank tensors made of momenta of vector bosons. The expression for the HVV vertex is given by,

$$\begin{aligned} \Gamma_{HVV}^{\mu\nu}(p_1, p_2) = & g_V m_V \kappa_V g^{\mu\nu} - \frac{g}{m_W} [\lambda_{1V} (p_1^\nu p_2^\mu - g^{\mu\nu} p_1 \cdot p_2) \\ & + \lambda_{2V} (p_1^\mu p_1^\nu + p_2^\mu p_2^\nu - g^{\mu\nu} p_1 \cdot p_1 - g^{\mu\nu} p_2 \cdot p_2) \\ & - \tilde{\lambda}_V \epsilon^{\mu\nu\alpha\beta} p_{1\alpha} p_{2\beta}]. \end{aligned} \quad (1)$$

Here, p_1 and p_2 are the momenta of the vector bosons. The BSM parameters κ_V and $\lambda_{1V,2V}$ are associated with CP-even couplings, while $\tilde{\lambda}_V$ is associated with CP-odd coupling.

We consider electron-proton collider to probe the HZZ coupling in the neutral current (NC) process, $e^- p \rightarrow e^- H j + X$, while the HWW coupling in the charged current (CC) process, $e^- p \rightarrow \nu_e H j + X$. In a previous study [5], we analyzed the sensitivity of these couplings using the absolute value of azimuthal correlation ($|\Delta\phi|$) between two final state particles. Distinct Lorentz structures of the CP-even and CP-odd components of these couplings motivate us to explore new angular observables that could be sensitive to the individual components. Since the CC process has missing energy in the final state, whereas the NC process has an e^- in the final state, the latter provides flexibility to study various angular observables. In this letter, we present the sensitivity of angular observables to the HZZ coupling and constraints on the parameters associated with this coupling. This analysis is performed at the tree level in perturbation theory. To minimize theoretical uncertainties, we further incorporate next-to-leading (NLO) corrections to CC and NC processes in QCD. Previous studies [6, 7] have addressed NLO QCD corrections for CC and NC processes in the SM. In our work, we show the effect of NLO QCD correction on angular observables sensitive to BSM physics.

2. Angular Observables

In this work, we follow the parton level analysis performed in Ref. [5], where the signal and background processes are discussed in detail. Events are generated using `MadGraph`, with the electron and proton beam energies set to 60 GeV and 7 TeV, respectively. In the signal process, the decay of the Higgs boson is considered in its dominant decay channel, $H \rightarrow b\bar{b}$. The signal is identified with e^- , two b-jets, and one light jet, $j = u, c, d, s, g$.

The angular distributions described in Eq. 2, defined in the lab frame, are as follows: θ_e represents the angle between the scattered electron (e^-) and the incident electron beam direction.

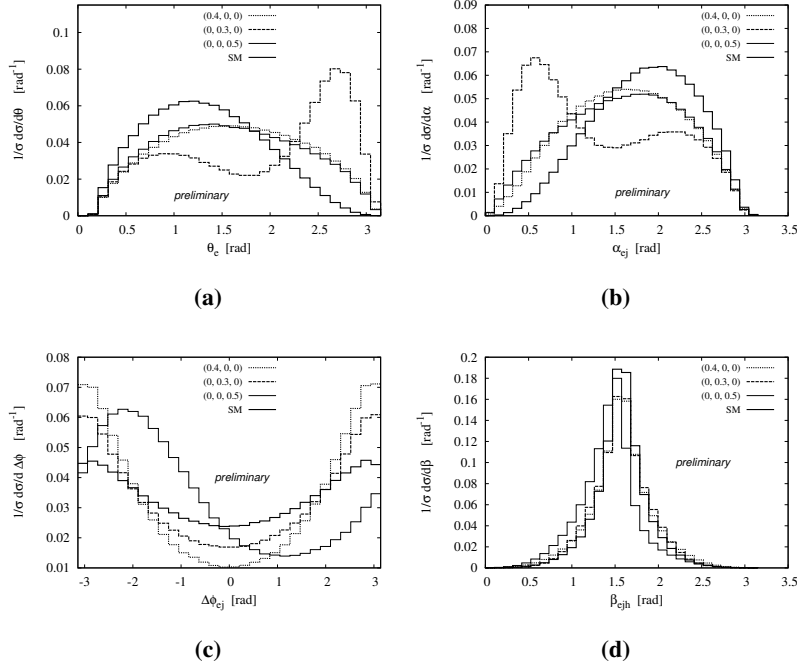


Figure 1: Angular observables for SM and benchmark values of BSM parameters ($\lambda_{1Z}, \lambda_{2Z}, \tilde{\lambda}_Z$) in the NC process.

The angle α_{ej} is the angle formed between the e^- and the jet . Lastly, β_{ejh} denotes the angle between the Higgs boson and the normal to the plane defined by the e^- and the jet .

$$\begin{aligned} \theta_e &= \cos^{-1} \left(\frac{\vec{p}_e \cdot \hat{z}}{|\vec{p}_e|} \right), & \alpha_{ej} &= \cos^{-1} \left(\frac{\vec{p}_e \cdot \vec{p}_j}{|\vec{p}_e| |\vec{p}_j|} \right) \\ \Delta\phi_{ej} &= \tan 2^{-1} \left(\frac{p_{ey}}{p_{ex}} \right) - \tan 2^{-1} \left(\frac{p_{jy}}{p_{jx}} \right), & \beta_{ejh} &= \cos^{-1} \left(\frac{(\vec{p}_e \times \vec{p}_j) \cdot \vec{p}_h}{|\vec{p}_e \times \vec{p}_j| |\vec{p}_h|} \right) \end{aligned} \quad (2)$$

Here, \vec{p}_i ($i = e, j, h$) are the momenta of final state particles: e^- , Higgs, and jet in the NC process. Fig. 1 shows the sensitivity of angular observables to individual BSM coupling. For demonstration, we use the benchmark values $\lambda_{1Z} = 0.4$, $\lambda_{2Z} = 0.3$, and $\tilde{\lambda}_Z = 0.5$ of these couplings. As shown in Fig. 1a, the polar angle θ_e is most sensitive to λ_{2Z} among all BSM couplings. We notice in Fig. 1b that the α_{ej} distribution efficiently distinguishes the λ_{2Z} coupling from the SM, while this distribution shows behavior similar to the SM for the other couplings, λ_{1Z} and $\tilde{\lambda}_Z$. The $\Delta\phi_{ej}$ distribution, as given in Eq. 2, is defined using the $\tan 2^{-1}$ (quadrant inverse tangent) function to consider all possible directions in the transverse plane of the detector. We notice in Fig. 1c that the $\Delta\phi_{ej}$ distribution is most sensitive to $\tilde{\lambda}_Z$. As shown in Fig. 1d, the β_{ejh} distribution is shifted towards left about $\beta_{ejh} = \pi/2$ for $\tilde{\lambda}_Z$ hence providing better sensitivity to this coupling.

We give constraints on BSM parameters based on the most sensitive angular observables. The χ^2 analysis is used by taking bins size of 9° in the distributions to estimate constraints on individual parameters. Fig. 2 presents the constraints on these couplings at a luminosity of 0.1 ab^{-1} and 2σ confidence level. The θ_e distribution is most sensitive to λ_{2Z} , while the $\Delta\phi_{ej}$ and β_{ejh} distributions

are most sensitive to $\tilde{\lambda}_Z$, we give constraints on λ_{2Z} and $\tilde{\lambda}_Z$ using the θ_e and $\Delta\phi_{ej}$ (or β_{ejh}) distributions, respectively. We compare these constraints with those from our previous analysis based on $|\Delta\phi_{ej}|$. We find that using these new angular observables, the constraints on λ_{2Z} and $\tilde{\lambda}_Z$ are narrowed down by $\sim 57\%$ compared to the constraints obtained from $|\Delta\phi_{ej}|$ in Ref. [5]. Further, we note that $|\Delta\phi_{ej}|$ is still the best observable to constrain λ_{1Z} .

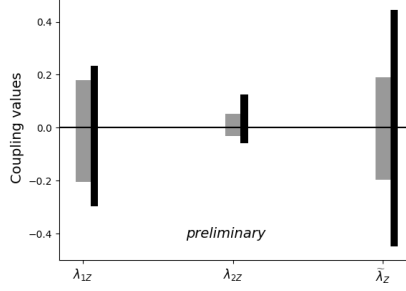


Figure 2: Constraints on angular observables from this study (grey bars) and from $|\Delta\phi_{ej}|$ distribution (black bars) of Ref. [5] which was based on a χ^2 analysis with two bins in the distribution. Constraints are obtained at 0.1 ab^{-1} luminosity and 2σ confidence level.

3. NLO QCD Corrections

We are interested in studying NLO QCD corrections on both NC and CC processes. Contribution at NLO requires virtual and real-emission corrections to the tree-level process, $e^-(k_1) q(p_b) \rightarrow e^-/\nu_e(k_2) H(p_H) q'(p_1)$. There is only one tree-level diagram and one virtual diagram at NLO. There are two sub-processes for the real emission diagrams and each subprocess has two real emission diagrams. The sub-processes are

$$e^-(k_1) q(p_b) \rightarrow e^-/\nu_e(k_2) q'(p_1) g(p_2) H(p_H) \quad (3)$$

$$e^-(k_1) g(p_b) \rightarrow e^-/\nu_e(k_2) q(p_1) \bar{q}'(p_2) H(p_H). \quad (4)$$

The virtual diagram is UV and IR divergent and we can write the exact expression for the virtual diagram in the t'Hooft-Veltman (HV) regularization scheme as

$$\mathcal{M}^V = \frac{\alpha_s(\mu_R)}{2\pi} \cdot \frac{(4\pi)^\epsilon}{\Gamma(1-\epsilon)} \cdot C_F \cdot \left(\frac{\mu^2}{t}\right)^\epsilon \cdot \left\{ -\frac{1}{\epsilon^2} - \frac{3}{2\epsilon} - 4 + \mathcal{O}(\epsilon) \right\} \times \mathcal{M}^B,$$

where \mathcal{M}^B is the born level amplitude. Here ϵ is defined as $\epsilon = (4-d)/2$, where d is the space-time dimension. $\alpha(\mu_R)$ is the strong coupling at renormalisation scale μ_R , and the color factor $C_F = 3/4$. The real emission diagrams are also divergent in the soft and collinear regions. The virtual and real amplitudes are separately divergent but their sum is finite. We adopt the Catani-Seymour dipole subtraction scheme following the Ref. [8] to handle the IR singularities. Following the reference, the NLO cross-section is written as,

$$\sigma^{\text{NLO}} = \int_{m+1} [d\sigma^R - \sum_{\text{dipoles}} d\sigma^B \otimes dV_{\text{dipole}}]_{\epsilon=0} + \int_m [d\sigma^V + d\sigma^B \otimes \mathbf{I}]_{\epsilon=0} \quad (5)$$

Here, σ^B , $d\sigma^V$, and σ^R are the Born, virtual, and real emission cross-sections. The \mathbf{I} term cancels all singularities in the virtual amplitude which has been regularised in d -dimension. The dipoles have the same point-like singular behavior as the real amplitudes in the soft and collinear regions. The two integrals in Eq. 5 are finite in 4-dimension and one can perform Monte-Carlo integration separately. For this process, the insertion operator \mathbf{I} can be written as

$$\mathbf{I}(\epsilon) = \frac{\alpha_s(\mu_R)}{2\pi} \cdot \frac{(4\pi)^\epsilon}{\Gamma(1-\epsilon)} \cdot 2C_F \cdot \left(\frac{\mu^2}{t}\right)^\epsilon \cdot \left\{ \frac{1}{\epsilon^2} + \frac{3}{2\epsilon} + 5 - \frac{\pi^2}{2} + \mathcal{O}(\epsilon) \right\}.$$

We have computed the dipoles for this process following the Ref. [8] and they show the exactly same behavior. To check the reliability of the calculation, we have compared the tree-level and real emission amplitude with MadGraph for a few sets of phase space points. We also compared the total cross section for leading order processes with MadGraph. All the checks are in agreement.

We use the CT18LO PDF set for LO calculations and CT18NLO for NLO calculations. The values of the SM parameters are as follows: the weak boson masses, $M_W = 80.3692$ GeV and $M_Z = 91.118$ GeV. Quark and lepton are taken as massless. The evolution of PDF and running of strong coupling depends on the renormalization (μ_R) and factorization (μ_F) scales. We set these scales equal to a dynamical scale as

$$\mu_R = \mu_F = \mu_0 = \frac{1}{3} \left(p_{T,l} + \sqrt{p_{T,H}^2 + M_H^2} + p_{T,j} \right).$$

We consider electron-proton collision with electron beam energy (E_e) = 60 GeV and proton beam energy (E_p) = 7 TeV. The total cross-section of NC and CC processes at LO (σ_0) and NLO (σ_{qcd}^{NLO}) are shown in the table given below.

Process	σ_0 (fb)	σ_{qcd}^{NLO} (fb)	RE (%)
$e^- p \rightarrow e^- H j$	17.44	18.25	4.6
$e^- p \rightarrow \nu_e H j$	91.86	96.55	5.1

The enhancement in the cross-section relative to LO, defined by RE, is 4.6% and 5.1% for the NC and CC processes, respectively. Since the diagrams involved in the QCD corrections for NC and CC processes are similar, the corrections are also similar in size. Fig. 3 demonstrates the effect of NLO corrections on the angular observables θ_e , α_{ej} , $\Delta\phi_{ej}$, and β_{ejh} distributions in the NC process of the SM in Higgs + 1 jet events. We observe that the θ_e and α_{ej} distributions exhibit flat corrections in the mid-region, while $\Delta\phi_{ej}$ and β_{ejh} show nontrivial corrections from QCD. This suggests that QCD corrections may be important for constraints on $\tilde{\lambda}_Z$.

4. Conclusion

We show the potential of angular observables to probe the HZZ coupling at ep collider with a center of mass energy of ~ 1.3 TeV. The angular observables, α_{ej} and $\Delta\phi_{ej}$, put $\sim 57\%$ stronger bounds on λ_{2Z} and $\tilde{\lambda}_Z$ as compared to the $|\Delta\phi_{ej}|$ distribution. To improve precision, we calculate the QCD NLO corrections to both NC and CC processes. At NLO, enhancements of 4.6% and 5.1% are noted with respect to LO in the NC and CC processes. We also show the effects of NLO QCD corrections on the angular observables considered in this study.

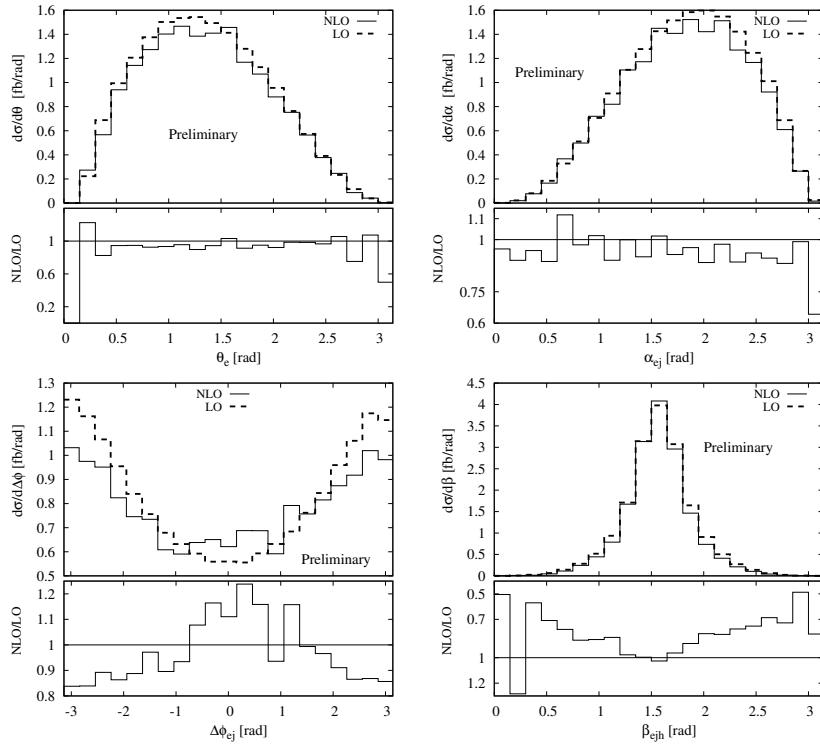


Figure 3: Angular distributions at LO and NLO for the NC process, $e^- p \rightarrow e^- H j$.

References

- [1] G. Aad *et al.* [ATLAS], Phys. Lett. B **716**, 1-29 (2012) doi:10.1016/j.physletb.2012.08.020 [arXiv:1207.7214 [hep-ex]].
- [2] S. Chatrchyan *et al.* [CMS], Phys. Lett. B **716**, 30-61 (2012) doi:10.1016/j.physletb.2012.08.021 [arXiv:1207.7235 [hep-ex]].
- [3] A. Tumasyan *et al.* [CMS], Nature **607**, no.7917, 60-68 (2022) [erratum: Nature **623**, no.7985, E4 (2023)] doi:10.1038/s41586-022-04892-x [arXiv:2207.00043 [hep-ex]].
- [4] G. Aad *et al.* [ATLAS], Nature **607**, no.7917, 52-59 (2022) [erratum: Nature **612**, no.7941, E24 (2022)] doi:10.1038/s41586-022-04893-w [arXiv:2207.00092 [hep-ex]].
- [5] P. Sharma and A. Shivaji, JHEP **10**, 108 (2022) doi:10.1007/JHEP10(2022)108 [arXiv:2207.03862 [hep-ph]].
- [6] J. Blumlein, G. J. van Oldenborgh and R. Ruckl, Nucl. Phys. B **395**, 35-59 (1993) doi:10.1016/0550-3213(93)90207-6 [arXiv:hep-ph/9209219 [hep-ph]].
- [7] B. Jager, Phys. Rev. D **81**, 054018 (2010) doi:10.1103/PhysRevD.81.054018 [arXiv:1001.3789 [hep-ph]].
- [8] S. Catani and M. H. Seymour, Nucl. Phys. B **485** (1997), 291-419 [arXiv:hep-ph/9605323 [hep-ph]].